International Journal of Nanomedicine

Dovepress
open access to scientific and medical research

Open Access Full Text Article

ORIGINAL RESEARCH

Preparation and Evaluation of Curcumin Derivatives Nanoemulsion Based on Turmeric Extract and Its Antidepressant Effect

Lin Sheng[1–4,*], Yumeng Wei[1,3,*], Chao Pi[1,3,*], Ju Cheng[3,4], Zhilian Su[1–4], Yuanyuan Wang[1,5], Tao Chen[1–4], Jie Wen[1–4], Yuxun Wei[1–4], Jingwen Ma[1–4], Jia Tang[1–4], Huiyang Liu[1–4], Zerong Liu[6,7], Hongping Shen[8], Ying Zuo[9], Wenwu Zheng[10], Ling Zhao[2–4]

[1]Key Laboratory of Medical Electrophysiology, Ministry of Education, School of Pharmacy of Southwest Medical University, Luzhou, People's Republic of China; [2]Luzhou Key Laboratory of Traditional Chinese Medicine for Chronic Diseases Jointly Built by Sichuan and Chongqing, the Affiliated Traditional Chinese Medicine Hospital of Southwest Medical University, Luzhou, Sichuan, People's Republic of China; [3]Key Laboratory of Medical Electrophysiology, Ministry of Education, Development Planning Department of Southwest Medical University, Luzhou, Sichuan, People's Republic of China; [4]Central Nervous System Drug Key Laboratory of Sichuan Province, School of Pharmacy of Southwest Medical University, Luzhou, Sichuan, People's Republic of China; [5]Department of Clinical Pharmacy, West China Hospital, Sichuan University, Chengdu, People's Republic of China; [6]Central Nervous System Drug Key Laboratory of Sichuan Province, Sichuan Credit Pharmaceutical CO., Ltd. Luxian County, Luzhou City, People's Republic of China; [7]Key Laboratory of Biorheological Science and Technology, Ministry of Education, College of Bioengineering, Chongqing University, Chongqing, 400030, People's Republic of China; [8]Clinical Trial Center, the Affiliated Traditional Chinese Medicine Hospital of Southwest Medical University, Luzhou, Sichuan, People's Republic of China; [9]Department of Comprehensive Medicine, the Affiliated Traditional Chinese Medicine Hospital of Southwest Medical University, Luzhou, Sichuan, People's Republic of China; [10]Department of cardiology, the Affiliated Hospital of Southwest Medical University, Luzhou, Sichuan, People's Republic of China

*These authors contributed equally to this work

Correspondence: Wenwu Zheng, Department of Cardiology, the Affiliated Hospital of Southwest Medical University, Luzhou, Sichuan, 646000, People's Republic of China, Tel/Fax +86 830 3165311, Email zhengwenwu888@163.com; Ling Zhao, Luzhou Key Laboratory of Traditional Chinese Medicine for Chronic Diseases Jointly Built by Sichuan and Chongqing, the Affiliated Traditional Chinese Medicine Hospital of Southwest Medical University, No. 182, Chunhui Road, Longmatan District, Luzhou, Sichuan, 646000, People's Republic of China, Tel/Fax +86 830 3160093, Email zhaoling@swmu.edu.cn

Purpose: The early stage of this study verified that a turmeric extract (TUR) including 59% curcumin (CU), 22% demethoxycurcumin (DMC), and 18% bisdemethoxycurcumin (BDMC), could enhance the stability of CU and had greater antidepressant potential in vitro. The objective of the study was to develop a nano-delivery system containing TUR (TUR-NE) to improve the pharmacokinetic behavior of TUR and enhance its antidepressant effect.

Methods: The antidepressant potential of TUR was explored using ABTS, oxidative stress-induced cell injury, and a high-throughput screening model. TUR-NE was fabricated, optimized and characterized. The pharmacokinetic behaviors of TUR-NE were evaluated following oral administration to normal rats. The antidepressant effect of TUR-NE was assessed within chronic unpredictable mild stress model (CUMS) mice. The behavioral and biochemical indexes of mice were conducted.

Results: The results depicted that TUR had 3.18 and 1.62 times higher antioxidant capacity than ascorbic acid and CU, respectively. The inhibition effect of TUR on ASP+ transport was significantly enhanced compared with fluoxetine and CU. TUR-NE displayed a particle size of 116.0 ± 0.31 nm, polydispersity index value of 0.121 ± 0.007, an encapsulation rate of 98.45%, and good release and stability in cold storage. The results of pharmacokinetics indicated the $AUC_{(0-t)}$ of TUR-NE was 8.436 and 4.495 times higher than that of CU and TUR, while the C_{max} was 9.012 and 5.452 times higher than that of CU and TUR, respectively. The pharmacodynamic study confirmed that the superior antidepressant effect of TUR-NE by significantly improving the depressant-like behaviors and elevating the content of 5-hydroxytryptamine in plasma and brain in CUMS mice. TUR-NE showed good safety with repeated administration.

Conclusion: TUR-NE, which had small and uniform particle size, enhanced the bioavailability and antidepressant effect of TUR. It could be a promising novel oral preparation against depression.

Keywords: turmeric extract, curcuminoids, nanoemulsion, stability, antidepressant effect, 5-hydroxytryptamine

Received: 15 July 2023
Accepted: 20 November 2023
Published: 27 December 2023

Introduction

Depression is a common mental disease that seriously endangers human physical and mental health. According to a World Health Organization (WHO) report, nearly 3 million people worldwide experience depression, constituting 4.4% of the global population.[1] Depression leads to severe mental and economic burdens on individuals, families, and society due to its high recurrence and disability.[2,3] However, the antidepressants currently in use generally have the disadvantages of significant side effects, slow effects, and recurrence.[4–6] In recent years, natural medicine has been widely utilized for studying the central nervous system because of its multi-component, multi-target, and multi-pharmacological effects.[7,8] Among them, curcumin (CU) is a polyphenol product extracted from the dried rhizome of turmeric.[9] It has been demonstrated to possess antidepressant activity in various animal models and clinical trials.[10–13] Studies revealed that CU could improve depressive symptoms in a variety of ways, including increasing 5-hydroxytryptamine (5-HT), dopamine (DA), and brain-derived neurotrophic factor (BDNF) levels within the hippocampus of rats.[14] Although the efficacy and safety of CU are promising, the poor stability and low oral bioavailability restrict its clinical application.[15–17]

Studies indicated that CU was more stable when it was present with two other major bioactive components of turmeric, namely, demethoxycurcumin (DMC) and bisdemethoxycurcumin (BDMC).[18,19] This suggested that CU could be more stable in turmeric extract, containing 59% CU, 22% DMC, and 18% BDMC. TUR might be more beneficial as a potential antidepressant than CU alone. The base degradation experiment and antidepressant studies were carried out in vitro in the early stage to verify the benefits of TUR. DMC and BDMC significantly enhanced the stability of CU. TUR had better antioxidant activity and provided a certain degree of neuronal protection compared to CU. The high-throughput screening model indicated that TUR might be involved in partial 5-HT reuptake inhibition.

TUR still has some problems, including low solubility and poor absorption, irrespective of its advantages in improving the stability of CU. Among the many strategies to improve the oral bioavailability of insoluble drugs, nanoemulsion (NE) could be an effective carrier for insoluble drugs. Moreover, it can strengthen the solubility, permeability, and stability of the drug at target sites, and the oral bioavailability of bioactive ingredients can be significantly enhanced using lipophilicity and nanoscale size.[20–22] Therefore, for the first time, this study used an emulsification method to develop an oral TUR delivery nanoemulsion (TUR-NE) to improve water solubility and oral bioavailability. The method was simple and reproducible and could be utilized in industrial production. The pharmacokinetic behavior of TUR-NE was also analyzed, and a chronic unpredictable mild stress (CUMS) animal model was established to assess the antidepressant activity of TUR-NE. These provided a theoretical basis and process to develop novel antidepressant drugs clinically.

Material and Methods

Materials

CU, DMC and BDMC were procured from Chengdu Best Reagent Co., Ltd. Chengdu, China. Turmeric extract (TUR) was obtained from Ruibo Technology Co., Ltd., China. Polyethylene glycol (PEG)-400, methanol (AR), ethanol (AR), and hydrochloric acid (AR) were provided by Cologne Chemicals Ltd. (Chengdu, China). We purchased fluoxetine hydrochloride, medium chain triglyceride (MCT), soy lecithin and Tween 80 from Shanghai Aladdin Bio-Chem Technology Co. Ltd., Shanghai, China. 3-(4,5-dimethylthiazol-2-yl)-2,5-diphenyltetrazolium bromide (MTT) were purchased from Beijing Solebao Technology Co., Ltd., China. Fetal bovine serum (FBS) and RPMI (Roswell Park Memorial Institute)-1640 were acquired from Beijing Thermo Fisher Scientific Shier Co., Ltd.

Cell Lines and Animals

PC12 cells were obtained from the cell bank of the Chinese Academy of Sciences (Shanghai, China) and cultured using RPMI 1640 medium with 10% (v/v) FBS and 1% (w/v) penicillin/streptomycin in an incubator containing 5% CO_2 at 37°C.

Sprague Dawley (SD) rats (age 8 to 9 weeks; 200 ± 20 g) were supplied by the Laboratory Animal Center of Southwest Medical University. The rats were housed in a pathogen-free environment with free access to water and food. C57BL/6 mice (age five weeks; male; 20 ± 3 g) were purchased from the Tengxin Technology Laboratory Animal Co., Ltd., Chongqing, China (approval number: SCXK(Jing) 2019–0010). Animal feeding occurred at a temperature of 20 ±

2°C and relative humidity of 40–60% in the SPF room of Laboratory Animal Center of Southwest Medical University. The Animal Protection and Use Committee of Southwest Medical University, Luzhou, Sichuan, China, approved the experimental procedures (No. 2020335).

The Stability of CU in TUR

Moderate amounts of pure CU, DMC, BDMC, and TUR were prepared in methanol to concentrations of 1, 0.4, 0.4, and 1 mg/mL, respectively. The buffer solution (pH 9) was comprised of Tris(hydroxymethyl)methyl aminomethane-hydrochloric acid and 40% ethanol. CU (1.5 mL) and 0.3, 0.6, 1, and 1.5 mL of DMC and BDMC were added to 4 25 mL amber volumetric flasks. CU was used as the control. One mL of TUR was added to another volume flask. The buffer solution was diluted to 25 mL and placed in a water bath at a constant temperature of 25°C. Finally, samples were taken at 20, 80, 140, 200, 260, 320, and 380 min.

The samples were analyzed using an Agilent 1260 high-performance liquid chromatography (HPLC) system (Agilent Technologies, Foster City, CA, USA) and an Inertsil ODS-SP C18 chromatographic column (4.2 mm × 250 mm; 5 μm; GL Sciences, Tokyo, Japan) with a Phenomenex C18 protective pre-column (4.0 mm × 3.0 mm). Samples were filtered through 0.22 μm syringe filters before injection. The mobile phase consisted of phosphoric acid (pH 3.5): acetonitrile (45:55, v/v) and was pumped at an 0.8 mL/min flow rate. The injection volume was 20 μL. The ultraviolet detection wavelength was 425 nm, and the column temperature was maintained at 30°C. The concentration of CU (C) was determined, and the degradation curves were obtained by plotting log C against time.

Study on Antidepressant Effect in vitro

The Antioxidant Activity of TUR

The antioxidant capacity of TUR was measured based on a previous study.[23] 2,2'-Azino-bis(3-ethylbenzothiazoline-6-sulphonic acid) radical (ABTS) solution (dissolved in 2.45 mM potassium persulfate) was primarily diluted using phosphoric acid buffer (pH 7.4) to 0.70 ± 0.02 absorbance. Then, 150 μL of CU, TUR, and vitamin C at different concentrations were transferred to 450 μL of ABTS solution. After reacting in the dark for 20 min, the samples were placed in a 96-well plate at 734 nm to measure the absorbance (A) of each concentration in triplicate. Anhydrous ethanol was used as the control. The calculation formula was:

$$\text{clearance rate}(\%) = \frac{\text{control A} - \text{sample A}}{\text{control A}} \times 100 \quad (1)$$

The Neuroprotective Effect of TUR

The PC12 cells in the logarithmic growth phase were inoculated in 96-well plates at a density of 5×10^3 cells/well and cultured for 24 h. After the supernatant was discarded, complete medium containing different concentrations of CU and TUR (3.75, 7.5, and 15 μg/mL) was added. Fluoxetine hydrochloride was utilized as the reference standard. The same amount of complete medium was added to the control and model groups. The supernatant was discarded after culturing for 12 h. Medium (100 μL) containing hydrogen peroxide (H_2O_2, 100 μM) was added to each well, and the same complete medium was added to the control group.[24] After 24 h, 5 mg/mL of MTT solution was added and incubated for 3 h. The absorbance of each well (A) was determined at 490 nm after the purple formazan product was dissolved in 150 μL of dimethyl sulfoxide (DMSO). The calculation formula was as follows:

$$\text{Cell viability}(\%) = \frac{\text{administration group A} - \text{blank group A}}{\text{control group A} - \text{blank group A}} \times 100 \quad (2)$$

The High-Throughput Screening Model

4-(4-(Dimethylamino)styryl)-n-methylpyridiunium (ASP+) was used to evaluate the inhibitory effect of TUR on the cellular uptake of ASP+ according to previous studies.[25] In the early stage, the appropriate ASP+ concentration was screened by assessing the inhibitory effect of fluoxetine hydrochloride. After PC12 cells adhered to the well wall, the medium was replaced with serum-free medium. After 4 h, fluoxetine hydrochloride was added, and the cells were

cultured for 2 h. Then, 10 μL of different concentrations of ASP+ dye were added and incubated for 1 h under dark conditions. Finally, the cells were washed twice using the D-Hanks solution. A microplate analyzer was utilized to detect and record the results at an excitation wavelength of 475 nm and an emission wavelength of 605 nm.

The concentrations in the CU and TUR groups were 3.75-60 μg/mL, and there were five parallel holes in each concentration group. After administration and incubation for 2 h, 10 μL ASP+ dye was added and the above steps were followed. Finally, the results of the fluorescence intensity were statistically analyzed.

Preparation of TUR-NE

TUR-NE was prepared by the mature emulsification method of our research group with minor adjustments.[26] In short, PEG-400, lecithin, MCT, and TUR were ultrasonically dissolved in ethanol as the oil phase. Tween 80 was ultrasonically dissolved in ultrapure water, constituting the water phase. Then, the oil phase was added to the water phase drop-by-drop under high-temperature stirring, and a clarified emulsion was obtained after cooling.

The preparation process (the temperature and time of emulsification and stirring speed) and conditions (the dosage of PEG-400, lecithin, MCT, Tween 80, absolute ethanol, ultrapure water, and TUR) were investigated by analyzing encapsulation efficiency (EE), particle size, and polydispersity index (PDI) as indexes to optimize the desirable NE characteristics. Three parallel samples were used for in each batch.

Optimization of TUR-NE

Central composite design response surface methodology (CCD-RSM) was applied based on single-factor experiments to optimize the TUR-NE formulation.[27,28] The dosage of Tween 80 (X_1), absolute ethanol (X_2), MCT (X_3), and lecithin (X_4), which greatly affected the physicochemical properties of NE, were taken as independent variables. EE (Y_1) and PDI (Y_2) were the response values to be optimized. Design-Expert 8.0 software was used to design the CCD scheme, consisting of 29 runs. The independent variables with the actual experimental level code values are shown in Table 1.

Characterization of TUR-NE

After diluting with deionized water, particle size, PDI, and the zeta potential of TUR-NE were measured using a Zetasizer Nano ZS (Malvern Instruments, Malvern, UK). The TUR-NE content was determined by HPLC to calculate EE and loading efficiency (LE). To this end, the prepared TUR-NE was centrifuged at 8000 rpm for 10 min, 50 μL of supernatant was taken, demulsified with methanol, and ultrasonicated for 10 min (200 W, 40 HZ), and the content of CU in NE was determined after filtration through a 0.22 um hydrophobic microporous membrane. In addition, the total CU content in TUR-NE was determined by HPLC at 425 nm. The following formula was utilized in the calculation:

$$\mathrm{EE}(\%) = \frac{\mathrm{Wd} - \mathrm{Wf}}{\mathrm{Wd}} \times 100 \tag{3}$$

$$\mathrm{LE}(\mathrm{mg/ml}) = \frac{\mathrm{Wd} - \mathrm{Wf}}{\mathrm{Wv}} \tag{4}$$

Ps: Where Wd is the amount of total CU in NE, Wf is the amount of free CU in NE, and Wv is the total volume of NE.

Table 1 The Independent Variables with the Actual Values of Their Experimental Level Codes

Independent Variables	Level		
	−1	0	+1
Tween 80 (X_1)	200	275	350
Absolute ethanol (X_2)	150	200	250
MCT (X_3)	300	350	400
Lecithin (X_4)	100	150	200

After staining with 1% phosphotungstic acid for 2 min, the morphology of the optimized TUR-NE was characterized by transmission electron microscopy (TEM, JEM-1400FLASH, Tokyo, Japan).

In vitro Release Study

The in vitro release of TUR and TUR-NE was studied by a dialysis method, as previously reported, with slight modification.[29] A TUR suspension and 1 mL of TUR-NE (containing equal amounts of TUR) were added to dialysis bags (MW 12000 D) and then placed in release medium (HCl, pH 1.2 and phosphate-buffered saline (PBS), pH 7.4, both containing 2% Tween 80) at a temperature of 37°C and a stirring rate of 100 rpm. One mL of release medium was removed at the specified times (0.25, 0.5, 1, 2, 4, 6, 8, 10, 12, 24, and 48 h), and the same amount of fresh release medium (37°C) was added. The CU content in samples was determined by HPLC, and the accumulating release was calculated.

Stability Study

Three batches of TUR-NE were stored at 25°C and 4°C for four months. The relative changes in particle size, PDI, EE, and LE of TUR-NE during storage were detected.

Pharmacokinetics Evaluation

Fifteen SD rats were randomly divided into three groups and given 100 mg/kg of CU, TUR, and TUR-NE (equivalent CU) by gavage. Blood samples were collected at 10, 30, 60, 120, 240, 360, 480, and 720 min. CU was extracted from the collected plasma using a mixture of ethyl acetate and methanol (9:1, v/v). The supernatant extracted twice was dried by nitrogen and redissolved in acetonitrile. Finally, the samples were analyzed by HPLC. The plasma concentration-time curves for each group were plotted, and the pharmacokinetic parameters were calculated using DAS 2.1.1 software.

Evaluation of Antidepressant Effect in vivo

Chronic Unpredictable Mild Stress Model (CUMS)

C57BL/6 mice were familiarized with the experimental environment for one week before the experiment. Then, they were divided into the control group (3 mice/cage) and CUMS group. The latter was exposed to one stressor (appearing in random order) every day. Similar stressors did not appear continuously, and the specific stressors were as follows: 4°C ice water bath for 5 min, 45°C hot water bath for 5 min, restraint for 6 h, day and night reversal, wet pad material for 24 h, oscillation for 15 min, noise for 1 h, and food and water deprivation for 24 h.[30] The CUMS group mice were raised in isolation, significantly elevating the anxiety and depression levels along with cognitive effects.[31] The outline of CUMS modeling and other experimental designs is depicted in Figure 1.

Drugs and Grouping

After applying stress, the mice were subjected to behavioral tests. The depressive-like mice, which were screened by the sucrose preference test (SPT) and forced swimming test (FST), were randomly divided into the CUMS group (normal saline, n = 6), positive control group (fluoxetine hydrochloride 20 mg/kg, n = 6), TUR group (100 mg/kg TUR, n = 6), TUR-NE group (100 mg/kg TUR, n = 6), and control group (normal saline every day). Behavioral tests were performed after 20 days of continuous administration.

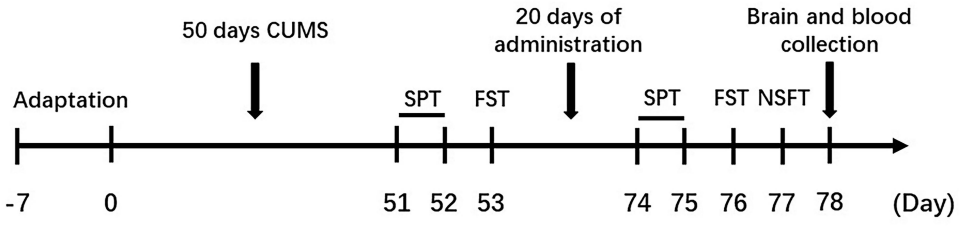

Figure 1 The experimental timeline.

Sucrose Preference Test

The SPT was performed as previously described.[32] The mice were acclimatized in cages using sucrose solution water bottles (1%, w/v) for 12 h, and then were deprived of water for 12 h. The mice were then placed in cages with two water bottles containing 1% sucrose solution and clean tap water. Sucrose solution and tap water consumption were recorded for 12 h, and the sucrose preference value was calculated using the following formula:

$$\text{Sucrose preference}(\%) = \frac{\text{Sucrose consumption}}{\text{Sucrose consumption} + \text{Water consumption}} \times 100 \quad (5)$$

Forced Swimming Test

In FST, the mice were placed inside a transparent glass tank (diameter 14 cm, height 20 cm) with tap water (25°C, water depth 10 cm) and timed for 6 min. The immobility time, defined as floating upright, except for occasional limb movements to keep the head afloat in the water, was recorded after 1 min of adaptation.[33]

Novelty-Suppressed Feeding Test

The novelty-suppressed feeding test (NSFT) was conducted as previously described.[34] After food deprivation overnight, the mice were kept in an open field (50 cm × 50 cm × 50 cm) in the same corner, with minimal food in the center. The test lasted for 10 min, and the time from entering the box to eating with a forepaw to ingesting food was recorded. At the end of each test, the field was cleaned using 75% ethanol. Noise and other interferences were minimized during the test.

Measurement of 5-HT and Monoamine Oxidase

Blood samples of the mice were collected and centrifuged (5000 rpm, 3 min) after the behavior tests. The supernatant was removed and stored at −80°C. Mice brains were rapidly removed after blood collection. The brain tissue samples were stored at −80°C after cleaning with pre-cooled normal saline. The concentration of 5-HT and monoamine oxidase (MAO) in the plasma and brain tissues was analyzed using commercial enzyme-linked immunosorbent assay (ELISA) kits. All experimental steps were performed according to the kit instructions, and absorbance was measured at 450 nm.

Histopathological Analysis

The heart, liver, and kidney tissues of the mice were collected immediately after the behavioral test and placed in 10% formaldehyde fixative for hematoxylin and eosin (H&E) staining. The study aimed to reveal the histopathological characteristics and injury to the heart, liver, and kidney of mice treated using TUR and TUR-NE for a short time. After dehydration, the tissues were embedded in paraffin, cut into 5-μm coronal sections, and stained with H&E. The BA210 digital trinocular microscopic camera system (MOTIC, Xiamen, China) was used to obtain slice images.

Statistical Analysis

All data were processed using GraphPad Prism 6.0 software and presented as means ± standard deviation (SD). Differences between groups were assessed by one-way analysis of variance. Post-hoc multiple comparisons were performed with the Student's *t* test. P values of < 0.05 was considered to be statistically significant.

Results

The Stability of CU in TUR

Based on the linear relationship shown in Figure 2A, the degradation of CU in TUR and the mixture containing different proportions of CU, DMC and BDMC could be described by first-order kinetics. The slope change indicated that the degradation rate of CU in TUR was slower than that in the mixture with other ratios, and the degradation rate of pure CU was the fastest. These findings revealed that the presence of DMC and BDMC in turmeric extract could enhance the stability of CU within an alkaline environment. The degree of improvement was associated with the proportion of the compound in the extract. The results indicated that TUR showed the best effect on slowing the degradation of CU compared with the mixture containing different proportions of CU, DMC, and BDMC.

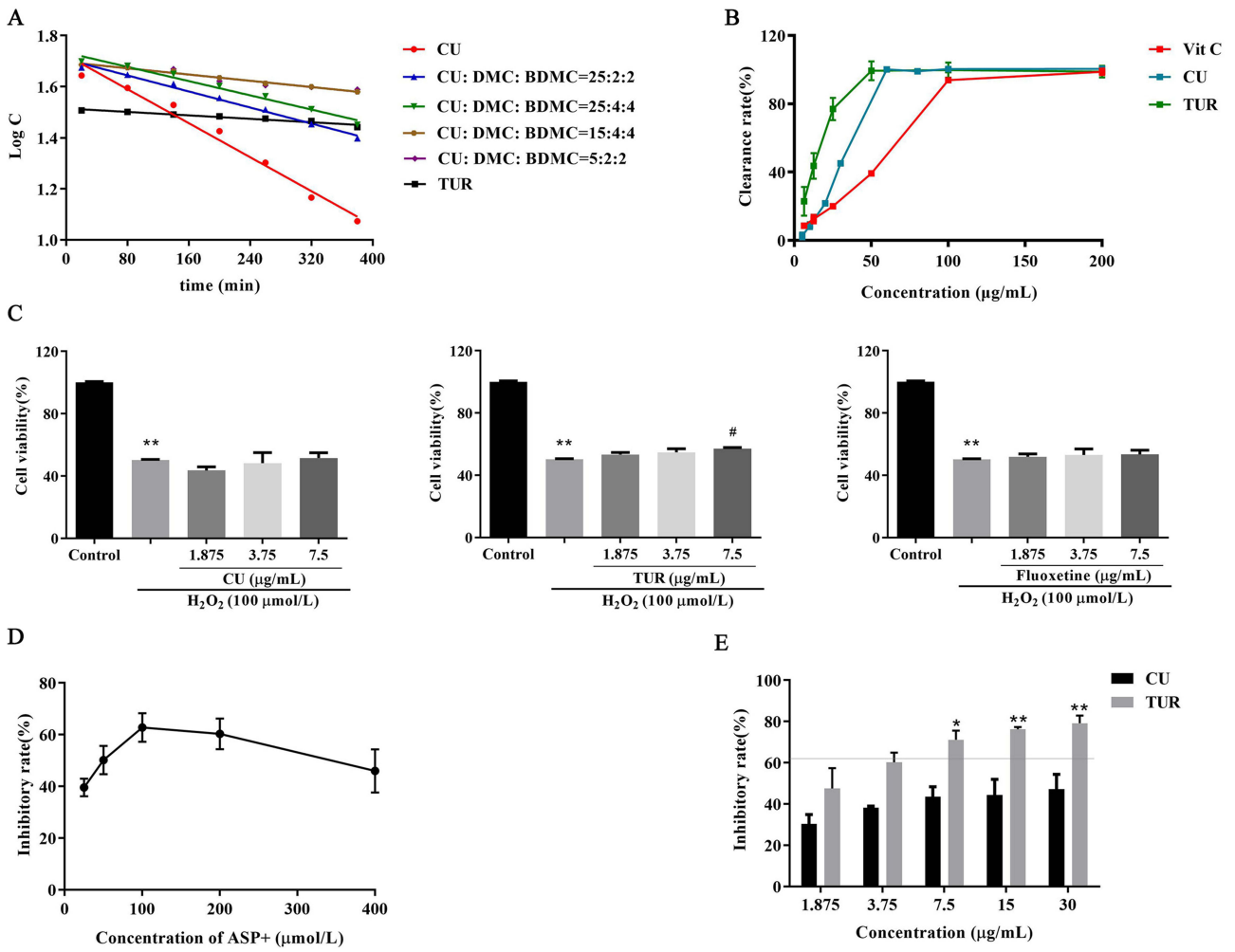

Figure 2 (**A**) Degradation curves of CU in mixtures of CU, DMC and BDMC with different ratios and in TUR. (**B**) The effect of Vit C, CU and TUR solution on scavenging ability of ABTS•+ radicals. (**C**) The protective effects of CU, TUR and fluoxetine hydrochloride on H_2O_2-induced cell injury model. Compared with control group: **P < 0.05, compared with H_2O_2 group: $^{\#}$P < 0.05. (**D**) The inhibition rate of fluoxetine hydrochloride on different concentrations of ASP+. (**E**) The inhibition rate of CU and TUR on ASP+. The line: the inhibition rate of fluoxetine hydrochloride on 100 μM ASP+. Compared with fluoxetine hydrochloride on ASP+: *P < 0.05, **P< 0.01.

The Antioxidant Capacity of TUR

The ABTS method was used to analyze the scavenging ability of ABTS•+ radicals by different concentrations of CU and TUR to study their antioxidant capacity. The data are represented in Figure 2B. All three substances had a scavenging effect on ABTS•+ radicals. The effect became more potent with increasing concentrations until it reached a stationary value. According to the IC_{50} values (17.94 μg/mL for TUR > 29.07 μg/mL for CU > 56.96 μg/mL for vitamin C), TUR had the highest antioxidant capacity, and the potential was significantly higher than that of CU.

The Neuroprotective Effect of TUR

Figure 2C shows that the cell survival rate of the model group was 50.38 ± 0.29% at 100 μM H_2O_2. It significantly differed from that of the control group (P < 0.01). There were no significant differences between low, medium, and high CU concentrations (43.59 ± 2.21%, 48.28 ± 6.81%, and 51.50 ± 3.48%, respectively) compared to the model group. The same was true for low and medium TUR concentrations (53.27 ± 1.25% and 54.32 ± 2.49%) and fluoxetine hydrochloride. The cell survival rate of the high-concentration TUR group (56.44 ± 1.67%) was 1.11 times higher than that of the CU group (compared with the model group, P < 0.05). These results indicated that a high concentration of TUR exerted a certain degree of neuroprotective effects because of its antioxidant capacity.

The High-Throughput Screening Model

As shown in Figure 2D, fluoxetine hydrochloride strongly inhibited 25–400 μM ASP+. The inhibition rate of fluoxetine hydrochloride became the highest (62.8%) when the dose of ASP+ reached 100 μM. Therefore, 100 μM ASP+ was chosen for the subsequent experiments.

Figure 2E shows that CU and TUR could inhibit ASP+ entry into cells in a concentration-dependent manner. However, the inhibition rate of CU was lower than that of TUR and fluoxetine hydrochloride. The inhibition rate of 7.5–30 μg/mL TUR showed good effects at medium and high concentrations (71.11 ± 4.42%, 76.21 ± 1.10%, and 79.12 ± 3.76%), which were significantly different from fluoxetine hydrochloride ($P < 0.05$ or $P < 0.01$). Fluoxetine hydrochloride exerted an antidepressant effect by increasing the concentration of 5-HT in the synaptic gap. Simultaneously, TUR had an inhibitory effect similar to or better than that of fluoxetine hydrochloride in the high-throughput screening model.

Single-Factor TUR-NE Experiments

The formulation and preparation process of TUR-NE were investigated by single-factor experiments. Firstly, the emulsification temperature, time, and stirring speed were determined, which were the key factors for the preparation of TUR-NE. As shown in Table 2, the indexes were better when the emulsification temperature and time were 70°C and 10 min, respectively, and the stirring speed was 500 rpm. Then, single factors of the formulation were investigated. The effects of the amount of oil phase, emulsifier, co-emulsifier, dissolvent, and TUR on the preparation of TUR-NE are shown in Table 3. Through a comprehensive analysis of the effect of EE, particle size, and PDI values, the formulation was as follows: the oil phase, 350 mg of PEG-400, 150 mg of lecithin, 350 mg of MCT, 25 mg of TUR, and 200 μL absolute ethanol; The water phase, 300 mg of Tween 80 and 2 mL of ultrapure water.

Further Optimization of TUR-NE

The results of the single-factor experiments showed that PEG-400 and TUR had little impact on EE, particle size, and the PDI value at 300–500 mg and 15–30 mg, respectively. Therefore, taking EE (Y_1) and the PDI value (Y_2) as response values, Tween 80 (X_1), absolute ethanol (X_2), MCT (X_3), and lecithin (X_4) were selected as variables. Design-Expert 8.0 was used in the CCD optimization experiment with four-factor and two levels. The generated 29 formulations and the observed response values are shown in Table 4. The fitting equations of Y_1 and Y_2 are shown below after performing multiple linear regression and polynomial equation fitting of the data:

$$Y_1 = 97.56 + 5.73 \times A + 3.44 \times B + 2.64 \times C - 10.52 \times D + 0.66 \times AB - 4.53 \times AC + 1.48 \times AD - 4.11 \times BC + 1.15 \times BD + 1.08 \times CD - 5.88 \times A^2 - 4.10 \times B^2 + 0.39 \times C^2 - 12.84 \times D^2$$

$$Y_2 = 0.14 - 0.10 \times A - 0.047 \times B - 0.076 \times C + 0.22 \times D - 0.032 \times AB + 0.022 \times AC - 0.065 \times AD - 0.019 \times BC - 0.11 \times BD - 0.14 \times CD + 0.063 \times A^2 + 0.054 \times B^2 + 0.047 \times C^2 + 0.22 \times D^2$$

Table 5 summarizes the results of the analysis of variance (ANOVA) for Y_1 and Y_2. The regression equations for EE and the PDI were statistically significant ($P < 0.0001$ for Y_1 and $P = 0.0003$ for Y_2). It revealed that all four selected

Table 2 Single Factor Analysis of the TUR-NE Preparation Process

		EE (%)	Size (nm)	PDI
Emulsification temperature (°C)	50	80.61 ± 3.78	865.3 ± 1.62	0.406 ± 0.03
	60	87.53 ± 3.75	125.4 ± 0.56	0.319 ± 0.02
	70	91.81 ± 1.42	137.1 ± 0.32	0.231 ± 0.01
Emulsification time (min)	5	93.83 ± 0.62	240.1 ± 0.69	0.083 ± 0.02
	10	95.52 ± 0.93	101.2 ± 0.52	0.234 ± 0.02
	20	90.38 ± 1.38	104.1 ± 1.16	0.262 ± 0.01
Speed (rpm)	250	94.43 ± 2.09	118.6 ± 0.76	0.240 ± 0.06
	500	95.95 ± 0.93	103.2 ± 0.13	0.213 ± 0.06
	800	77.68 ± 1.85	133.3 ± 0.88	0.155 ± 0.02

Table 3 Single Factor Analysis of the TUR-NE Prescription

		EE (%)	Size (nm)	PDI
PEG-400 (mg)	300	92.20 ± 0.41	163.1 ± 0.23	0.294 ± 0.02
	350	98.14 ± 0.31	101.9 ± 0.74	0.229 ± 0.05
	400	97.95 ± 1.30	117.2 ± 0.74	0.266 ± 0.02
	450	96.52 ± 0.93	123.3 ± 0.52	0.269 ± 0.06
	500	96.07 ± 1.12	136.5 ± 0.13	0.275 ± 0.06
Lecithin (mg)	75	97.29 ± 0.40	279.0 ± 14.00	0.654 ± 0.25
	100	98.23 ± 0.40	240.0 ± 2.06	0.518 ± 0.21
	150	98.98 ± 0.45	105.3 ± 0.56	0.204 ± 0.12
	200	95.56 ± 1.20	120.2 ± 0.46	0.823 ± 0.32
	250	92.03 ± 1.87	141.0 ± 5.78	1.000 ± 0.85
MCT (mg)	250	96.33 ± 1.90	110.4 ± 0.32	0.624 ± 0 0.23
	300	97.05 ± 0.81	112.7 ± 1.00	0.495 ± 0.11
	350	98.74 ± 0.49	103.5 ± 0.79	0.203 ± 0.01
	400	93.78 ± 1.02	313.2 ± 0.46	0.246 ± 0.02
	450	92.70 ± 0.25	376.2 ± 1.07	0.254 ± 0.06
Tween 80 (mg)	100	77.97 ± 2.09	391.4 ± 0.82	0.584 ± 0.12
	150	87.05 ± 2.06	147.1 ± 0.57	0.482 ± 0.09
	200	91.03 ± 1.86	140.4 ± 0.14	0.451 ± 0.02
	250	94.52 ± 0.85	116.8 ± 0.68	0.322 ± 0.04
	300	96.52 ± 0.93	92.52 ± 0.13	0.269 ± 0.02
TUR (mg)	15	96.19 ± 0.42	101.9 ± 0.737	0.244 ± 0.01
	20	97.95 ± 0.75	108.0 ± 0.615	0.229 ± 0.01
	25	97.20 ± 1.01	122.7 ± 0.519	0.156 ± 0.03
	30	98.18 ± 0.89	138.0 ± 0.191	0.179 ± 0.04
	40	90.80 ± 0.73	259.5 ± 0.76	0.234 ± 0.06
Absolute ethanol (μL)	25	86.56 ± 1.63	40.05 ± 3.70	0.542 ± 0.23
	50	89.19 ± 1.15	57.37 ± 0.44	0.524 ± 0.12
	100	90.95 ± 0.83	71.42 ± 0.77	0.439 ± 0.02
	150	95.66 ± 0.54	86.39 ± 2.45	0.356 ± 0.03
	200	97.89 ± 0.94	103.2 ± 0.74	0.236 ± 0.05
Ultrapure water (mL)	0.5	89.92 ± 0.60	816.3 ± 0.17	0.588 ± 0.26
	1.5	94.20 ± 0.04	756.0 ± 1.50	0.402 ± 0.12
	2.0	96.24 ± 0.31	120.1 ± 0.85	0.230 ± 0.01
	3.0	95.20 ± 0.56	942.0 ± 6.52	0.595 ± 0.23
	4.0	91.33 ± 0.11	992.0 ± 2.71	0.608 ± 0.32

formulation variables significantly influenced EE and PDI values. The R^2 values of the two response values were 0.9447 and 0.9246, respectively, and the difference between them and the adjusted R^2 values was less than 0.2, which confirmed the reliability of the polynomial regression model.[35] The response surface plots shown in Figure 3 illustrate the impact of the interaction of these four factors on EE and PDI values. The steeper fluctuation trend of the curves indicated that the variable factors had more obvious influence on the response values.[27,28] The final predicted formulation was Tween 80 (285.31 mg), absolute ethanol (206.88 μL), MCT (356.88 mg), and lecithin (147.50 mg).

Characterization of TUR-NE

The particle size, PDI, zeta-potential (Figure 4A and B), EE, and LE of TUR-NE prepared by the optimized formulation were 116.0 ± 0.305 nm, 0.121 ± 0.007, −11.6 ± 1.23 mV, 98.45 ± 0.31%, and 4.00 ± 0.361 mg/mL, respectively. The EE and PDI values were close to the predicted values (98.89% and 0.142), which indicated that the optimal formulation obtained by the CCD model was appropriate. The photomicrograph revealed that the droplet outlines of optimized TUR-NE were smooth and spherical (Figure 4C), and the size was consistent with the particle size measured above.

Table 4 Experimental Design and the Experimental Values of Response Variables

Number	X_1 (mg)	X_2 (mg)	X_3 (mg)	X_4 (mg)	Y_1 (%)	Y_2
1	200.00	150.00	350.00	150.00	82.03	0.438
2	350.00	150.00	350.00	150.00	92.03	0.195
3	200.00	250.00	350.00	150.00	80.01	0.471
4	350.00	250.00	350.00	150.00	92.62	0.101
5	275.00	200.00	300.00	100.00	97.52	0.113
6	275.00	200.00	400.00	100.00	95.22	0.201
7	275.00	200.00	300.00	200.00	71.20	0.982
8	275.00	200.00	400.00	200.00	75.03	0.524
9	200.00	200.00	350.00	100.00	82.99	0.247
10	350.00	200.00	350.00	100.00	94.09	0.200
11	200.00	200.00	350.00	200.00	60.23	0.775
12	350.00	200.00	350.00	200.00	77.02	0.467
13	275.00	150.00	300.00	150.00	82.20	0.352
14	275.00	250.00	300.00	150.00	98.87	0.242
15	275.00	150.00	400.00	150.00	96.44	0.266
16	275.00	250.00	400.00	150.00	96.87	0.080
17	200.00	200.00	300.00	150.00	79.36	0.368
18	350.00	200.00	300.00	150.00	97.46	0.187
19	200.00	200.00	400.00	150.00	98.23	0.179
20	350.00	200.00	400.00	150.00	98.19	0.085
21	275.00	150.00	350.00	100.00	86.02	0.169
22	275.00	250.00	350.00	100.00	96.42	0.278
23	275.00	150.00	350.00	200.00	65.20	0.681
24	275.00	250.00	350.00	200.00	80.20	0.367
25	275.00	200.00	350.00	150.00	98.56	0.117
26	275.00	200.00	350.00	150.00	97.10	0.130
27	275.00	200.00	350.00	150.00	97.77	0.148
28	275.00	200.00	350.00	150.00	97.64	0.141
29	275.00	200.00	350.00	150.00	96.73	0.152

Table 5 Analysis of Variance (ANOVA) for the Quadratic Model

Quadratic Model	R^2 value	Adjusted R^2	F-value	P-value
Y_1	0.9447	0.8894	22.14	< 0.0001
Y_2	0.9246	0.8492	11.30	0.0003

In vitro Release Study

Figure 4D shows the accumulated release of the TUR suspension and NE in two release mediums. The accumulative release rate of CU in TUR and TUR-NE in HCl within 48 h was 19.69 ± 0.65% and 36.51 ± 3.24%, whereas that in PBS was 21.90 ± 1.24% and 44.90 ± 2.47%, respectively. The results indicated that the accumulative release of CU from TUR-NE was higher than that from the TUR suspension.

Stability of TUR-NE

Figure 4E-H indicates that the particle size, PDI, EE, and LE of TUR-NE did not significantly change when stored at 4°C for 120 d. The appearance was still clear and transparent without precipitation. The particle size and PDI value gradually increased, and EE and LE gradually decreased after storage at 25°C for 15 d. These results indicated that TUR-NE had strong stability during cold storage.

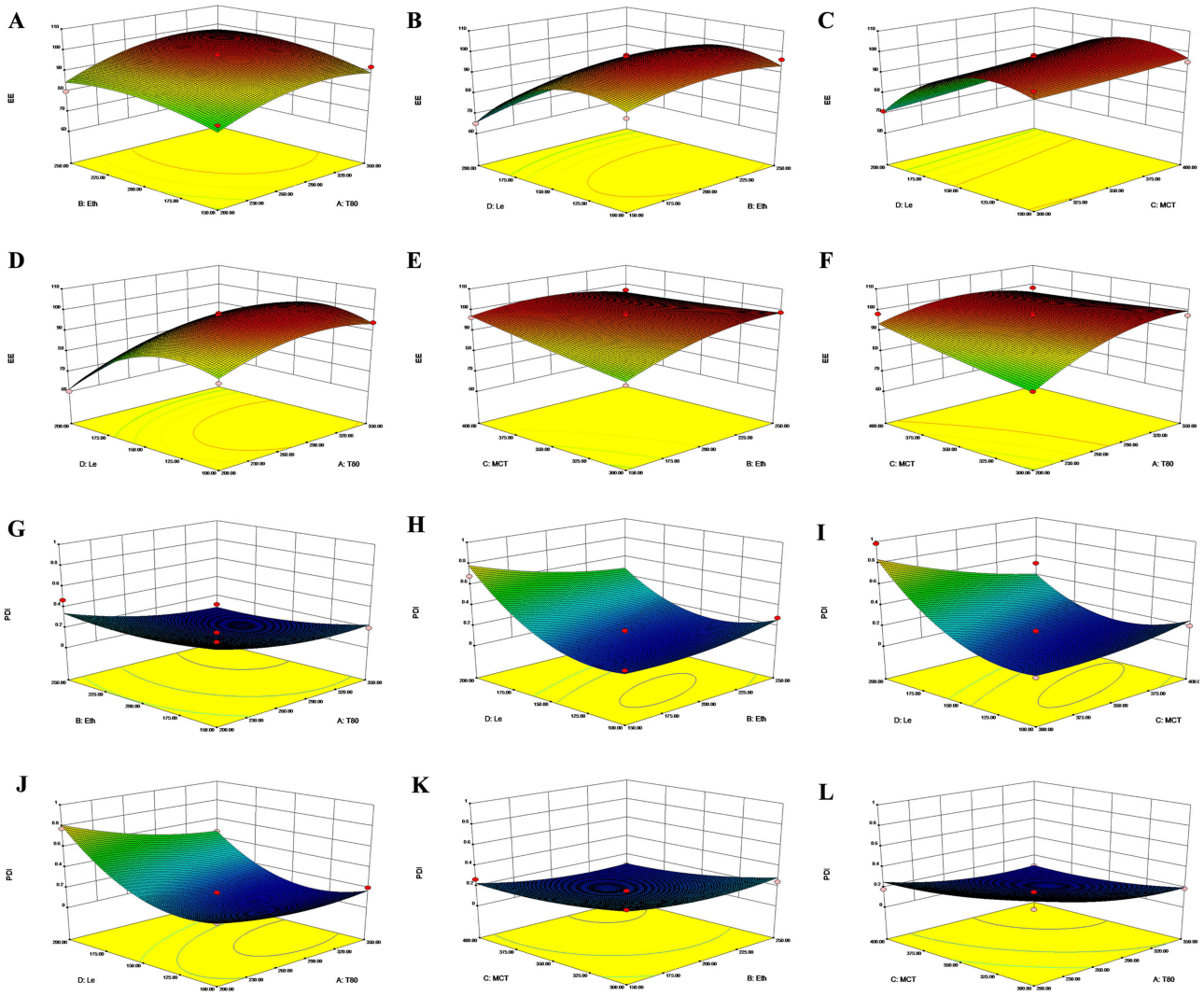

Figure 3 The response surface plots of the effect for the independent variable on EE (**A-F**) and PDI (**G-L**).

Pharmacokinetics of TUR-NE

The plasma concentration-time curves (Figure 5A) revealed that the plasma concentration of CU in the TUR group was higher after 60 min than that in the CU group. The plasma concentration of CU in the TUR-NE group was significantly higher than that in the CU and TUR groups at the same time point. Table 6 shows the pharmacokinetic parameters of each group. Compared to the CU and TUR groups, the TUR-NE group had a prominently elevated area under the curve ($AUC_{(0-t)}$), 8.436 times higher than that of the CU group and 4.495 times higher than that of the TUR group. The peak concentration (C_{max}) of the TUR-NE group was also higher than that of the CU and TUR groups, at 9.012 times and 5.452 times, respectively. However, the mean residence time ($MRT_{(0-t)}$) and $T_{1/2}$ of the TUR-NE group were slightly lower than those of the CU and TUR groups.

Effect of TUR-NE on the Behavior of CUMS Mice

Figure 5B shows that the sucrose preference of CUMS group mice (54.02 ± 12.91%) was significantly lower than that of control group mice (78.94 ± 12.85%, $P < 0.01$). In the FST (Figure 5C), the immobility time of the mice in the CUMS group was 146.95 ± 52.00 s, significantly higher than that of the control group ($P < 0.01$). Simultaneously, the mice showed untidy hair, dullness, and decreased spontaneous activity after chronic stress.

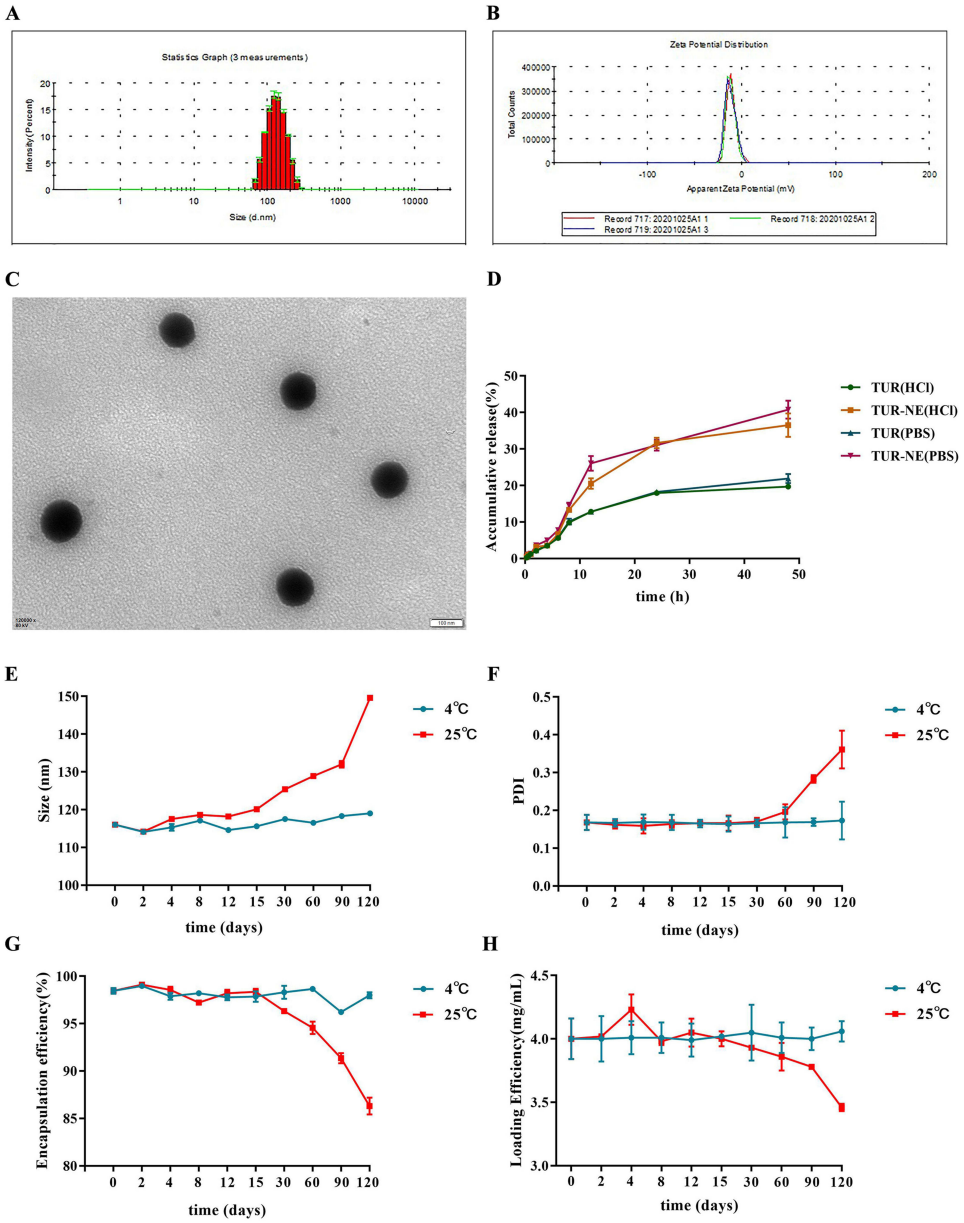

Figure 4 (**A**) Size and (**B**) Zeta potential of TUR-NE. (**C**) TEM image of TUR-NE (12,000 × magnification). (**D**) Accumulative release rate for TUR and TUR-NE in HCl (PH 1.2) and PBS (PH 7.4). The variation in (**E**) size, (**F**) PDI, (**G**) EE, and (**H**) LE of TUR-NE during stability study.

Figure 5D shows that the sucrose preference of the control and TUR-NE groups was 73.80 ± 13.27% and 77.50 ± 18.26%, respectively, significantly higher than that of CUMS group. In contrast, the TUR group showed no significant increase. There was no significant difference between control and TUR-NE groups. Figure 5E indicates that the FST immobility time of the mice in the TUR and TUR-NE groups was significantly lower than in the CUMS group ($P < 0.01$). Compared with the positive control group, the immobility time of TUR-NE group was significantly lower ($P < 0.05$). Additionally, the feeding latency in the NSFT in the CUMS group was 499.20 ± 94.80 s (Figure 5F), and reversed after a certain period of treatment with fluoxetine hydrochloride, TUR, and TUR-NE ($P < 0.05$).

Detection of 5-HT and MAO Activity

As shown in Figure 5G-J, the 5-HT content in the plasma and brain of mice in the CUMS group was 16.27 ± 1.12 ng/mL and 43.97 ± 0.45 ng/mL, respectively. It was significantly lower than in the control group ($P < 0.01$). After administering

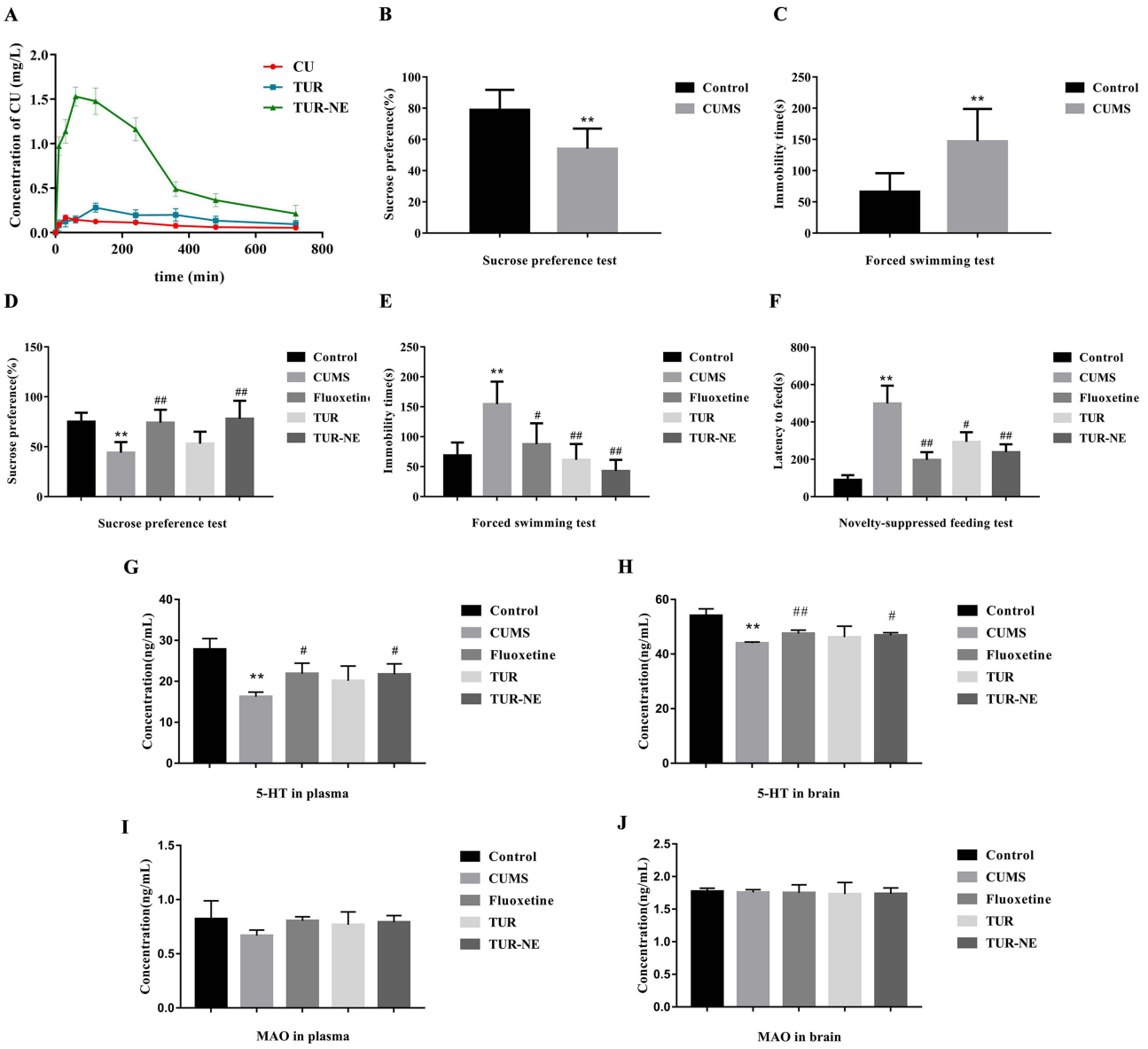

Figure 5 (**A**) The plasma concentration-time curves of CU after given CU, TUR, and TUR-NE by oral administration. (**B**) The sucrose preference value of the CUMS model mice in SPT. (**C**) The immobility time of the CUMS model mice in FST. (**D-F**) The depression-like and anxiety-like behaviors were improved after administration. (**D**) The sucrose preference value of the mice in SPT, (**E**) the immobility time of the mice in FST, (**F**) the latency time to feed of the mice in NSFT. (**G-J**) The levels of 5-HT and MAO in plasma and brain of the mice. Compared with control group: **P < 0.01, compared with CUMS model group: #P < 0.05, ##P < 0.01.

fluoxetine hydrochloride, TUR, TUR-NE, the 5-HT content in plasma was 21.89 ± 2.58 ng/mL, 20.16 ± 3.59 ng/mL, 21.70 ± 2.57 ng/mL, and in the brain, it was 47.54 ± 1.23 ng/mL, 46.19 ± 4.02 ng/mL, and 46.86 ± 0.99 ng/mL, respectively. The 5-HT in plasma and brain of fluoxetine hydrochloride and TUR-NE groups was significantly increased compared to the CUMS group ($P < 0.05$). There was no significant difference in the MAO content in plasma and brain tissue among the different groups.

Histological Analysis

H&E staining revealed (Figure 6) no noticeable lesions in the heart, liver, and kidney tissues of mice in the CUMS group. The hepatocyte cytoplasm was vacuolated inside some liver tissue. Mice in the fluoxetine hydrochloride and TUR-NE groups showed mild glomerular enlargement or renal tubule degeneration compared to the control group. The myocardial fibers in the fluoxetine hydrochloride group were slightly vacuolated but were not in the TUR and TUR-NE groups.

Table 6 The Main Pharmacokinetic Parameters of CU, TUR, and TUR-NE

	Unit	CU	TUR	TUR-NE
$AUC_{(0-t)}$	mg/L^{-1} ·min	63.341	118.879	534.363
$MRT_{(0-t)}$	min	290.448	314.971	235.029
$T_{1/2}$	min	352.539	456.397	300.181
T_{max}	min	30.000	120.000	60.000
CL	$L \cdot min^{-1} \cdot kg^{-1}$	1.208	0.554	0.160
C_{max}	mg/L	0.170	0.281	1.532

Abbreviations: $AUC_{(0-t)}$, area under the curve; $MRT_{(0-t)}$, the mean residence time; $T_{1/2}$, the half-life period; T_{max}, the time to peak concentration; CL, the clearance rate; C_{max}, the peak concentration.

Discussion

The poor stability and low oral bioavailability of CU are the main problems affecting its clinical application. Prior studies addressed the poor stability of CU by modifying the structure of CU or synthesizing different delivery systems. For instance, Fang et al[36] introduced a dimethylaminomethyl group to the ortho position of the hydroxy group, and the target compound had improved aqueous solubility and stability compared to CU, besides exerting potent antioxidant activity. CU liposomes and phospholipid complexes were also developed to enhance intracellular and targeted drug delivery.[37–39] DMC and BDMC were reported to synergistically enhance the bioactivity of CU when included in the curcuminoid mixture.[40] The alkaline degradation of curcumin is due to the deprotonation of hydroxyl groups and the self-oxidation of methoxy groups on phenyl rings. Among them, BDMC is resistant to auto-oxidation because of the lack of methoxy groups, so whether in pure or mixture forms, BDMC and DMC (one methoxy group) are more resistant to alkaline degradation than CU (two methoxy groups).[18] From these findings, it could be inferred that the presence of DMC and BDMC in curcuminoids might have reduced the degradation percentage of CU and themselves by their synergistic stabilizing effect. In the study, TUR was a curcuminoid with different ratios of the three components than previous commercial curcumin preparations. The stability exploration experiment confirmed that the presence of DMC and BDMC could enhance the stability of CU. Simultaneously, the study explored the correlation between this enhancement and the proportion of the three components. The stability effect was stronger when the ratio of CU, DMC, and BDMC was closer to that of TUR.

Compelling evidence indicated that the pathogenesis of depression was associated with neurotransmitter disorder, hypothalamic-pituitary-adrenal axis activity disorder, oxidative stress, and reduced neurotrophic factor concentrations.[41,42] CU has been increasingly utilized in antidepressant studies for its extensive antioxidant, anti-inflammatory and neuroprotective effects.[43] As an antioxidant, CU enhanced the activity of antioxidant enzymes, including superoxide dismutase and catalase, and decreased the concentration of oxidative stress markers, such as malondialdehyde and nitric oxide (NO).[44] In the study, the scavenging ability of TUR on ABTS•+ radicals and the protective effect on H_2O_2-induced PC12 cell oxidative damage were investigated to explore whether TUR had a similar or better antioxidant capacity and neuroprotective effects than those of CU.[45,46] The results revealed that TUR had a more substantial antioxidant capacity than CU or ascorbic acid. However, neither CU nor TUR significantly improved cell survival in a cell injury model. This might have been related to the solubility of CU and TUR. Nevertheless, the antioxidant capacity of TUR could still reduce cell damage caused by oxidative stress. Previous studies reported that CU could increase the concentration of 5-HT in the hippocampus, amygdala, and striatum of rats exposed to long-term stress.[47] To explore the regulatory effect of TUR on the serotonergic nervous system, ASP+ was utilized to quantify the uptake of 5-HT in PC12 cells. As a fluorescent analog of neurotoxin MPP+, ASP+ can replace 5-HT and bind to its transporter for cell uptake.[25,48] Fluoxetine hydrochloride is a reuptake inhibitor of 5-HT and can block this process.[49] The study showed that the inhibitory effect of CU was concentration-dependent, but it did not reach the effect of fluoxetine hydrochloride. Instead, the inhibition rate of TUR concentrations from 7.5–30 μg/mL was significantly higher than that

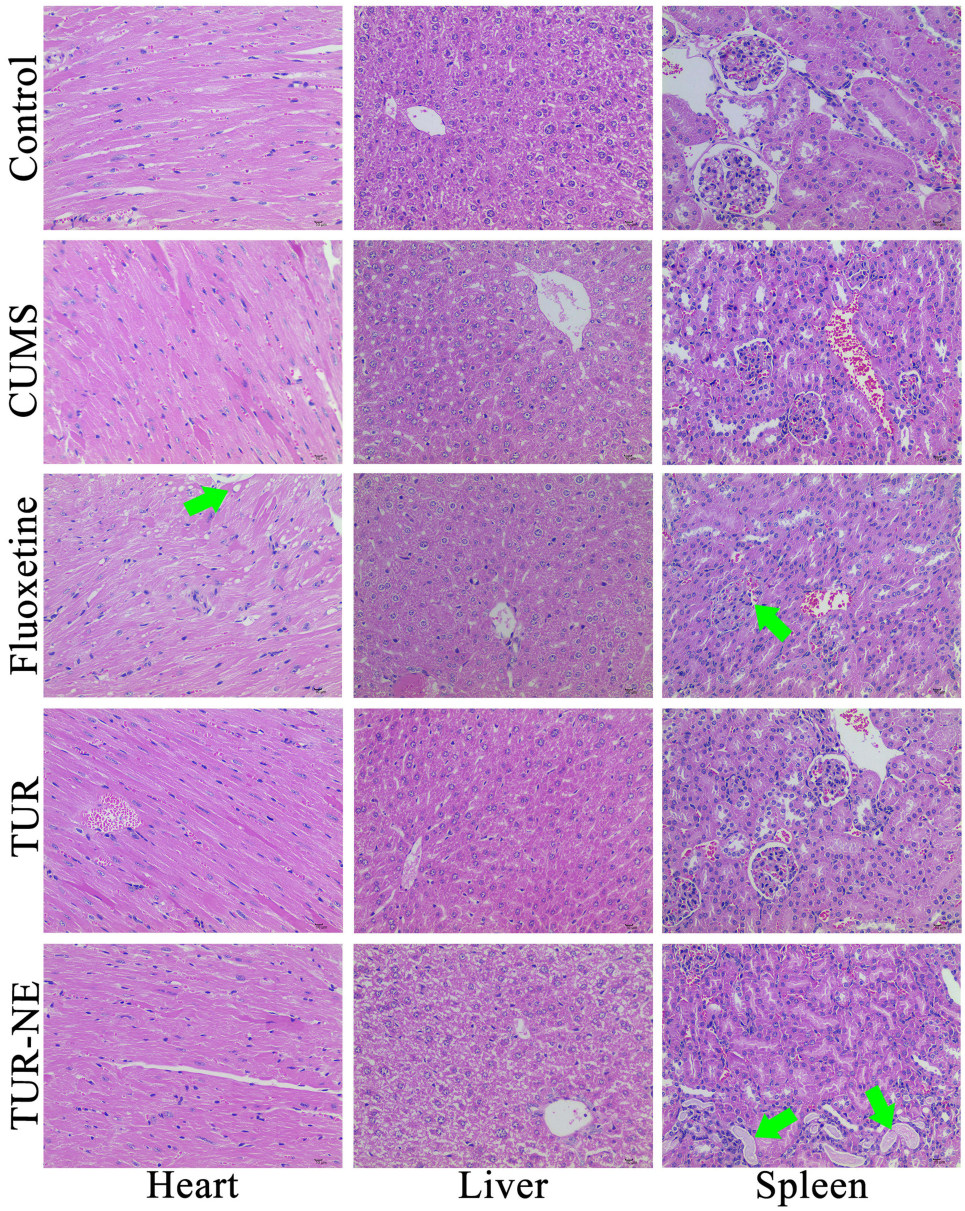

Figure 6 Pathological section images of heart, liver, and kidney in mice (400 × magnification). The green arrow: slight degeneration of the tissue organs.

of fluoxetine. These results indicated that the antioxidant capacity and inhibitory effect of TUR on 5-HT reuptake were significantly stronger than those of CU. Thus, TUR showed better antidepression potential than CU.

NE is a thermodynamically unstable isotropic system, which improves solubility and oral bioavailability by trapping raw drug material inside. As key evaluation indexes of NE, particle size, and PDI values are directly related to drug release, absorption, and dispersion.[50] Smaller droplet sizes and appropriate PDI values (< 0.3) can improve the uniformity and stability of drug particles and facilitate drug absorption.[51,52] In addition, a high drug EE value represents an excellent preparation process and high compatibility between drugs and excipients.[50,53] In this study, the optimized TUR-NE was small and uniform in size, with a high EE value, stable prescription, and excellent reproducibility. Lecithin, PEG-400, and Tween 80 can be utilized as surfactants and co-surfactants to make the droplets more stable in the whole system.[54] TUR-NE showed good release behavior in two mediums simulating the gastrointestinal tract status. Compared to free TUR, NE significantly improved the release of CU. This might be attributed to the appropriate drop size and the solubilizing ability of NE.[29,55] The main properties of TUR-NE remained stable for 120 days at 4°C. However, its EE

decreased slowly over time at room temperature after 15 days. In conclusion, the optimized TUR-NE had good characterization and could enhance drug release, thus increasing the bioavailability of TUR. Its stability under cold storage conditions made it suitable for future antidepression research and clinical application.

The co-existing curcuminoids could improve the bioavailability of CU.[56,57] Here, TUR also increased the plasma concentration of CU in rats to promote its absorption. TUR-NE further increased the C_{max} and $AUC_{(0-t)}$ of CU in rats based on free TUR. These effects could have been due to PEG-400 increasing the water solubility of TUR and passing through the gastrointestinal mucus in a smaller molecule state, which was more easily absorbed into the circulatory system.[58] However, the $MRT_{(0-t)}$ and $T_{1/2}$ of TUR-NE were slightly lower than those of CU and TUR, suggesting that the TUR-NE elevated hydrophilicity and accelerated drug metabolism.

CUMS is a classic animal model of depression that produces a series of physiological responses and abnormal behaviors similar to the depressive symptoms of humans.[59] The model is often used to evaluate the efficacy of antidepressants based on behavioral and biochemical tests.[60] Behavioral tests showed that mice in the CUMS group exhibited considerable depression-like and anxiety-like behaviors, consistent with previous studies.[29,61,62] After 20 days of administration, TUR and TUR-NE significantly improved depression-like and anxiety-like behaviors and increased the 5-HT content in the plasma and brain of chronically stressed mice, and TUR-NE could achieve the same effect as fluoxetine hydrochloride. The pathologic sections showed glomerular enlargement or degeneration in the fluoxetine group, and the TUR-NE group showed mild symptoms, not causing obvious pathological changes. A small amount of cytoplasmic vacuolization was found in some liver tissue, which was also observed in the control group. This was considered to be an increase in liver glycogen in the mice caused by insufficient fasting before dissection. The results indicated satisfactory safety of TUR and TUR-NE in vivo. TUR-NE could restore 5-HT levels by inhibiting its transporter by improving water solubility and oral bioavailability of the bulk drug. Simultaneously, the antioxidant capacity of TUR-NE might be involved in the process of antioxidative stress. A previous study showed that CU-coated iron oxide nanoparticles exerted antidepressant effects by inhibiting MAO activity and increasing the synthesis of monoamine neurotransmitters.[63] Although the present study did not find that increases in 5-HT levels were related to the effects of TUR-NE on its metabolism, they indicated that TUR-NE could play an antidepressant role by inhibiting 5-HT reuptake. More studies are needed to explore the specific mechanisms and verify our findings.

Conclusion

The stability of CU in TUR was significantly improved. The antidepressant potential of TUR in vitro was better than that of CU. TUR-NE was successfully developed and optimized with uniform and small particle sizes, which significantly enhanced the pharmacokinetic behavior of TUR in rats. TUR-NE obviously improved the depression and anxiety-like behaviors of CUMS mice and exerted antidepressant effects by regulating the serotonergic system. The antidepressant effect and relevant mechanism of TUR were preliminarily elucidated. Further studies are expected to shed light on the exact molecular mechanism and clinical applications.

Data Sharing Statement

The authors confirm that the data supporting the findings of this study are available within the article.

Ethical Approval Statement

During the experiment, all animals have well housing and husbandry, suffering was reduced and in accordance with humanitarianism. The animal studies were done in compliance with the regulations and guidelines of Southwest Medical University institutional animal care and adhered to the ARRIVE guidelines. The Animal Protection and Use Committee of Southwest Medical University, Luzhou, Sichuan, China, approved the experimental procedures (No. 2020335).

Acknowledgments

This study was supported by the central government guides the local science and technology development special fund (No.2022ZYD0084) and Key R&D projects (No.2022YFS0627) of the Science and Technology Department of Sichuan province of China, Key Research and Development Projectors of Luzhou (No.2022-SYF-85), the Research Fund

(No.210027-01SZ, 200017-01SZ, 230008-01SZ, 230007-01SZ) of Sichuan Province, Sichuan Credit Pharmaceutical CO., Ltd., Central Nervous System Drug Key Laboratory of Sichuan Province, Chongqing Traditional Chinese Medicine Inheritance and Innovation Team Construction Project "Traditional Chinese Medicine New Drug and Safety Research Inheritance and Innovation Team" (No. 2022-8).

Author Contributions

All authors made a significant contribution to the work reported, whether that is in the conception, study design, execution, acquisition of data, analysis and interpretation, or in all these areas; took part in drafting, revising or critically reviewing the article; gave final approval of the version to be published; have agreed on the journal to which the article has been submitted; and agree to be accountable for all aspects of the work.

Disclosure

The authors report no conflicts of interest in this work.

References

1. World Health Organization. Depression and Other Common Mental Disorders: global Health Estimates. 2017. Available from: https://apps.who.int/iris/handle/10665/254610. Accessed March 13, 2022.
2. Kennedy SH. Core symptoms of major depressive disorder: relevance to diagnosis and treatment. *Dialogues Clin Neurosci*. 2008;10(3):271–277. doi:10.31887/DCNS.2008.10.3/shkennedy
3. Kiyohara C, Yoshimasu K. Molecular epidemiology of major depressive disorder. *Environ Health Preventative Med*. 2009;14(2):71–87. doi:10.1007/s12199-008-0073-6
4. Jakobsen JC, Katakam KK, Schou A, et al. Selective serotonin reuptake inhibitors versus placebo in patients with major depressive disorder. A systematic review with meta-analysis and Trial Sequential Analysis. *BMC Psychiatry*. 2017;17:28. doi:10.1186/s12888-016-1173-2
5. Fornaro M, Anastasia A, Novello S, et al. The emergence of loss of efficacy during antidepressant drug treatment for major depressive disorder: an integrative review of evidence, mechanisms, and clinical implications. *Pharmacol Res*. 2019;139:494–502. doi:10.1016/j.phrs.2018.10.025
6. Gaynes B, Lux L, Gartlehner G, et al. Defining treatment-resistant depression. *Depression Anxiety*. 2020;37(2):134–145. doi:10.1002/da.22968
7. Rodriguez-Landa JF, German-Ponciano LJ, Puga-Olguin A, Olmos-Vazquez OJ. Pharmacological, Neurochemical, and Behavioral Mechanisms Underlying the Anxiolytic- and Antidepressant-like Effects of Flavonoid Chrysin. *Molecules*. 2022;27(11):17. doi:10.3390/molecules27113551
8. Lu J, Wang X, Wu AX, et al. Ginsenosides in central nervous system diseases: pharmacological actions, mechanisms, and therapeutics. *Phytother Res*. 2022;36(4):1523–1544. doi:10.1002/ptr.7395
9. Huang F, Cai X, Hou X, et al. A dynamic covalent polymeric antimicrobial for conquering drug-resistant bacterial infection. *Exploration*. 2022;2(5):20210145. doi:10.1002/EXP.20210145
10. Fusar-Poli L, Vozza L, Gabbiadini A, et al. Curcumin for depression: a meta-analysis. *Crit Rev Food Sci Nutr*. 2020;60(15):2643–2653. doi:10.1080/10408398.2019.1653260
11. Abu-Taweel GM, Al-Fifi Z. Protective effects of curcumin towards anxiety and depression-like behaviors induced mercury chloride. *Saudi J Biol Sci*. 2021;28(1):125–134. doi:10.1016/j.sjbs.2020.09.011
12. Marques JGD, Antunes FTT, Brum LFD, et al. Adaptogenic effects of curcumin on depression induced by moderate and unpredictable chronic stress in mice. *Behav Brain Res*. 2021;399:8. doi:10.1016/j.bbr.2020.113002
13. Rubab S, Naeem K, Rana I, et al. Enhanced neuroprotective and antidepressant activity of curcumin-loaded nanostructured lipid carriers in lipopolysaccharide-induced depression and anxiety rat model. *Int J Pharm*. 2021;603:13. doi:10.1016/j.ijpharm.2021.120670
14. Afzal A, Batool Z, Sadir S, et al. Therapeutic Potential of Curcumin in Reversing the Depression and Associated Pseudodementia via Modulating Stress Hormone, Hippocampal Neurotransmitters, and BDNF Levels in Rats. *Neurochem Res*. 2021;46(12):3273–3285. doi:10.1007/s11064-021-03430-x
15. Appendino G, Allegrini P, de Combarieu E, Novicelli F, Ramaschi G, Sardone N. Shedding light on curcumin stability. *Fitoterapia*. 2022;156:5. doi:10.1016/j.fitote.2021.105084
16. Anand P, Kunnumakkara AB, Newman RA, Aggarwal BB. Bioavailability of curcumin: problems and promises. *Mol Pharm*. 2007;4(6):807–818. doi:10.1021/mp700113r
17. Zhang J, Li S, An FF, et al. Self-carried curcumin nanoparticles for in vitro and in vivo cancer therapy with real-time monitoring of drug release. *Nanoscale*. 2015;7(32):13503–13510. doi:10.1039/c5nr03259h
18. Peram MR, Jalalpure SS, Palkar MB, Diwan PV. Stability studies of pure and mixture form of curcuminoids by reverse phase-HPLC method under various experimental stress conditions. *Food Sci Biotechnol*. 2017;26(3):591–602. doi:10.1007/s10068-017-0087-1
19. Wei MM, Zhao SJ, Dong XM, et al. A combination index and glycoproteomics-based approach revealed synergistic anticancer effects of curcuminoids of turmeric against prostate cancer PC3 cells. *J Ethnopharmacol*. 2021;267:113467. doi:10.1016/j.jep.2020.113467
20. Ramires OV, Alves BD, Barros PAB, et al. Nanoemulsion Improves the Neuroprotective Effects of Curcumin in an Experimental Model of Parkinson's Disease. *Neurotox Res*. 2021;39(3):787–799. doi:10.1007/s12640-021-00362-w
21. Rodriguez-Burneo N, Busquets MA, Estelrich J. Magnetic Nanoemulsions: comparison between Nanoemulsions Formed by Ultrasonication and by Spontaneous Emulsification. *Nanomaterials*. 2017;7(7):13. doi:10.3390/nano7070190
22. Zhang J, Nie W, Chen R, et al. Green Mass Production of Pure Nanodrugs via an Ice-Template-Assisted Strategy. *Nano Lett*. 2019;19(2):658–665. doi:10.1021/acs.nanolett.8b03043
23. Kose LP, Gulcin I. Evaluation of the Antioxidant and Antiradical Properties of Some Phyto and Mammalian Lignans. *Molecules*. 2021;26(23):15. doi:10.3390/molecules26237099

24. Minato T, Nakamura N, Saiki T, et al. β-Aminoisobutyric acid, L-BAIBA, protects PC12 cells from hydrogen peroxide-induced oxidative stress and apoptosis via activation of the AMPK and PI3K/Akt pathway. *IBRO Neurosci Rep*. 2021;12:65–72. doi:10.1016/j.ibneur.2021.12.001
25. Lau T, Proissl V, Ziegler J, Schloss P. Visualization of neurotransmitter uptake and release in serotonergic neurons. *J Neurosci Methods*. 2015;241:10–17. doi:10.1016/j.jneumeth.2014.12.009
26. Guo P, Pi C, Zhao SJ, et al. Oral co-delivery nanoemulsion of 5-fluorouracil and curcumin for synergistic effects against liver cancer. *Expert Opin Drug Deliv*. 2020;17(10):1473–1484. doi:10.1080/17425247.2020.1796629
27. Ye Q, Li J, Li T, et al. Development and evaluation of puerarin-loaded controlled release nanostructured lipid carries by central composite design. *Drug Dev Ind Pharm*. 2021;47(1):113–125. doi:10.1080/03639045.2020.1862170
28. Geng D, Li Y, Wang C, et al. Optimization, and in vitro and in vivo evaluation of etomidate intravenous lipid emulsion. *Drug Deliv*. 2021;28 (1):873–883. doi:10.1080/10717544.2021.1917729
29. Jang JH, Jeong SH, Lee YB. Enhanced Lymphatic Delivery of Methotrexate Using W/O/W Nanoemulsion: in vitro Characterization and Pharmacokinetic Study. *Pharmaceutics*. 2020;12(10):978. doi:10.3390/pharmaceutics12100978
30. Li HN, Xiang YJ, Zhu ZM, et al. Rifaximin-mediated gut microbiota regulation modulates the function of microglia and protects against CUMS-induced depression-like behaviors in adolescent rat. *J Neuroinflamm*. 2021;18(1):18. doi:10.1186/s12974-021-02303-y
31. Song MK, Lee JH, Kim YJ. Effect of chronic handling and social isolation on emotion and cognition in adolescent rats. *Physiol Behav*. 2021;237:7. doi:10.1016/j.physbeh.2021.113440
32. Xia J, Gu L, Guo YT, et al. Gut Microbiota Mediates the Preventive Effects of Dietary Capsaicin Against Depression-Like Behavior Induced by Lipopolysaccharide in Mice. *Front Cell Infect Microbiol*. 2021;11:13. doi:10.3389/fcimb.2021.627608
33. Martins J, Brijesh S. Anti-depressant activity of Erythrina variegata bark extract and regulation of monoamine oxidase activities in mice. *J Ethnopharmacol*. 2020;248:112280. doi:10.1016/j.jep.2019.112280
34. Zhou Y, Huang SH, Wu FL, et al. Atractylenolide III reduces depressive- and anxiogenic-like behaviors in rat depression models. *Neurosci Lett*. 2021;759:7. doi:10.1016/j.neulet.2021.136050
35. Kumar G, Virmani T, Pathak K, et al. Central Composite Design Implemented Azilsartan Medoxomil Loaded Nanoemulsion to Improve Its Aqueous Solubility and Intestinal Permeability: in vitro and Ex Vivo Evaluation. *Pharmaceuticals*. 2022;15(11):1343. doi:10.3390/ph15111343
36. Fang XB, Fang L, Gou SH, Cheng L. Design and synthesis of dimethylaminomethyl-substituted curcumin derivatives/analogues: potent antitumor and antioxidant activity, improved stability and aqueous solubility compared with curcumin. *Bioorg Med Chem Lett*. 2013;23(5):1297–1301. doi:10.1016/j.bmcl.2012.12.098
37. Sohn SI, Priya A, Balasubramaniam B, et al. Biomedical Applications and Bioavailability of Curcumin-An Updated Overview. *Pharmaceutics*. 2021;13(12):33. doi:10.3390/pharmaceutics13122102
38. Liang GA, Shao LL, Wang Y, et al. Exploration and synthesis of curcumin analogues with improved structural stability both in vitro and in vivo as cytotoxic agents. *Bioorg Med Chem*. 2009;17(6):2623–2631. doi:10.1016/j.bmc.2008.10.044
39. Omidi S, Rafiee Z, Kakanejadifard A. Design and synthesis of curcumin nanostructures: evaluation of solubility, stability, antibacterial and antioxidant activities. *Bioorganic Chem*. 2021;116:9. doi:10.1016/j.bioorg.2021.105308
40. Anand P, Thomas SG, Kunnumakkara AB, et al. Biological activities of curcumin and its analogues (Congeners) made by man and Mother Nature. *Biochem Pharmacol*. 2008;76(11):1590–1611. doi:10.1016/j.bcp.2008.08.008
41. Zhou BT, Zhu ZQ, Ransom BR, Tong XP. Oligodendrocyte lineage cells and depression. *Mol Psychiatr*. 2021;26(1):103–117. doi:10.1038/s41380-020-00930-0
42. Kowalczewski PL, Olejnik A, Rybicka I, Zielinska-Dawidziak M, Bialas W, Lewandowicz G. Membrane Filtration-Assisted Enzymatic Hydrolysis Affects the Biological Activity of Potato Juice. *Molecules*. 2021;26(4):11. doi:10.3390/molecules26040852
43. Bhat A, Mahalakshmi AM, Ray B, et al. Benefits of curcumin in brain disorders. *Biofactors*. 2019;45(5):666–689. doi:10.1002/biof.1533
44. Lopresti AL. Potential Role of Curcumin for the Treatment of Major Depressive Disorder. *CNS Drugs*. 2022;36(2):123–141. doi:10.1007/s40263-022-00901-9
45. Roma E, Mattoni E, Lupattelli P, et al. New Dihydroxytyrosyl Esters from Dicarboxylic Acids: synthesis and Evaluation of the Antioxidant Activity In Vitro (ABTS) and in Cell-Cultures (DCF Assay). *Molecules*. 2020;25(14):3135. doi:10.3390/molecules25143135
46. Kang J, Wang Y, Guo X, et al. N-acetylserotonin protects PC12 cells from hydrogen peroxide induced damage through ROS mediated PI3K / AKT pathway. *Cell Cycle*. 2022;21(21):2268–2282. doi:10.1080/15384101.2022.2092817
47. Lee B, Lee H. Systemic Administration of Curcumin Affect Anxiety-Related Behaviors in a Rat Model of Posttraumatic Stress Disorder via Activation of Serotonergic Systems. *Evid-Based Complement Altern Med*. 2018;2018:12. doi:10.1155/2018/9041309
48. Babu DK, Diaz A, Samikkannu T, et al. Upregulation of Serotonin Transporter by Alcohol in Human Dendritic Cells: possible Implication in Neuroimmune Deregulation. *Alcoholism*. 2009;33(10):1731–1738. doi:10.1111/j.1530-0277.2009.01010.x
49. Zhu HJ, Appel DI, Grundemann D, Richelson E, Markowitz JS. Evaluation of organic cation transporter 3 (SLC22A3) inhibition as a potential mechanism of antidepressant action. *Pharmacol Res*. 2012;65(4):491–496. doi:10.1016/j.phrs.2012.01.008
50. Pandey P, Gulati N, Makhija M, Purohit D, Dureja H. Nanoemulsion: a Novel Drug Delivery Approach for Enhancement of Bioavailability. *Recent Pat Nanotechnol*. 2020;14(4):276–293. doi:10.2174/1872210514666200604145755
51. Mura P, Maestrelli F, D'Ambrosio M, et al. Evaluation and Comparison of Solid Lipid Nanoparticles (SLNs) and Nanostructured Lipid Carriers (NLCs) as Vectors to Develop Hydrochlorothiazide Effective and Safe Pediatric Oral Liquid Formulations. *Pharmaceutics*. 2021;13(4):437. doi:10.3390/pharmaceutics13040437
52. Ho TM, Abik F, Mikkonen KS. An overview of nanoemulsion characterization via atomic force microscopy. *Crit Rev Food Sci Nutr*. 2022;62 (18):4908–4928. doi:10.1080/10408398.2021.1879727
53. Li K, Pi C, Wen J, et al. Formulation of the novel structure curcumin derivative-loaded solid lipid nanoparticles: synthesis, optimization, characterization and anti-tumor activity screening in vitro. *Drug Deliv*. 2022;29(1):2044–2057. doi:10.1080/10717544.2022.2092235
54. Chuacharoen T, Prasongsuk S, Sabliov CM. Effect of Surfactant Concentrations on Physicochemical Properties and Functionality of Curcumin Nanoemulsions Under Conditions Relevant to Commercial Utilization. *Molecules*. 2019;24(15):12. doi:10.3390/molecules24152744
55. Wang J, Chen H, Guo T, et al. Isoliquiritigenin Nanoemulsion Preparation by Combined Sonication and Phase-Inversion Composition Method: in vitro Anticancer Activities. *Bioengineering (Basel)*. 2022;9(8):382. doi:10.3390/bioengineering9080382

56. Li R, Qiao X, Li Q, et al. Metabolic and pharmacokinetic studies of curcumin, demethoxycurcumin and bisdemethoxycurcumin in mice tumor after intragastric administration of nanoparticle formulations by liquid chromatography coupled with tandem mass spectrometry. *J Chromatogr B Analyt Technol Biomed Life Sci*. 2011;879(26):2751–2758. doi:10.1016/j.jchromb.2011.07.042
57. Saadati S, Sadeghi A, Mansour A, et al. Curcumin and inflammation in non-alcoholic fatty liver disease: a randomized, placebo controlled clinical trial. *BMC Gastroenterol*. 2019;19(1):133. doi:10.1186/s12876-019-1055-4
58. Wang YY, Pi C, Feng XH, Hou Y, Zhao L, Wei YM. The Influence of Nanoparticle Properties on Oral Bioavailability of Drugs. *Int J Nanomed*. 2020;15:6295–6310. doi:10.2147/ijn.S257269
59. Jia HM, Feng YF, Liu YT, et al. Integration of H-1 NMR and UPLC-Q-TOF/MS for a Comprehensive Urinary Metabonomics Study on a Rat Model of Depression Induced by Chronic Unpredictable Mild Stress. *PLoS One*. 2013;8(5):11. doi:10.1371/journal.pone.0063624
60. Peng ZL, Zhang C, Yan L, et al. EPA is More Effective than DHA to Improve Depression-Like Behavior, Glia Cell Dysfunction and Hippcampal Apoptosis Signaling in a Chronic Stress-Induced Rat Model of Depression. *Int J Mol Sci*. 2020;21(5):17. doi:10.3390/ijms21051769
61. Zhang K, Wang ZQ, Pan X, Yang JY, Wu CF. Antidepressant-like effects of Xiaochaihutang in perimenopausal mice. *J Ethnopharmacol*. 2020;248:7. doi:10.1016/j.jep.2019.112318
62. Zhang SS, Tian YH, Jin SJ, et al. Isoflurane produces antidepressant effects inducing BDNF-TrkB signaling in CUMS mice. *Psychopharmacology*. 2019;236(11):3301–3315. doi:10.1007/s00213-019-05287-z
63. Khadrawy YA, Hosny EN, Magdy M, et al. Antidepressant effects of curcumin-coated iron oxide nanoparticles in a rat model of depression. *Eur J Pharmacol*. 2021;908:174384. doi:10.1016/j.ejphar.2021.174384